SUPPLEMENTAL OMIP-070: NKp46-based 27-color panel to define Natural Killer cells isolated from human tumor tissues

Marie Frutoso, Florian Mair, Martin Prlic

Developmental Strategy

1. Panel development

Instrument configuration

This 27-color panel was developed for a FACSymphony A5 with the configuration specified in **Online Table 1**. Markers were grouped based on priority. The highest priority was assigned to assess the viability of the cells. Including a marker of viability is required as dead cells have greater autofluorescence and increased non-specific binding that can affect the quality of the staining (1). The L/D fixable blue dead cell stain kit (referred to as UV L/D) was used, since not a lot of antibodies are available coupled to the AF350 fluorochrome to date.

	Laser	Power	Name	Mirror	Bandpass	Flurochrome used
1	355nm	65mW	U395		379/28	BUV395
2			U450	410LP	450/50	UV L/D
3			U500	470LP	515/30	BUV496
4			U570	550LP	570/30	BUV563
5			U660	635LP	660/40	BUV660
6			U740	710LP	640/35	BUV737
7			U780	755LP	785/62	BUV805
8	405nm	200mW	V450		450/40	BV421
9			V510	505LP	515/20	BV480
10			V570	550LP	575/25	BV570
11			V605	580LP	605/20	BV605
12			V655	630LP	660/20	BV650
13			V710	685LP	710/40	BV711
14			V750	735LP	750/30	BV750
15			V780	770LP	785/62	BV786
16	488nm	200mW	B515	505LP	515/20	FITC
17			B610	600LP	610/20	BB630
18			B660	635LP	660/40	BB660
19			B710	695LP	710/50	BB700
20			B780	750LP	780/40	BB790
21	532nm	200mW	G575		575/25	PE
22			G610	600LP	610/20	PE-CF594
23			G660	635LP	660/40	PE-Cy5
24			G710	690LP	710/50	PE-Cy5.5
25			G780	750LP	780/60	PE-Cy7
26	628nm	200mW	R660		670/30	eFluor660
27			R710	685LP	730/45	AF700
28			R780	750LP	780/45	APC-H7

Online Table 1: Instrument Configuration

The BD FACSymphony A5 used for this panel development is equipped with 7 detectors for the 355nm Ultra Violet (UV) laser, 8 detectors for the 405nm violet laser, 5 detectors for both the 488nm blue and 532nm green lasers, and 3 detectors for the 628nm red laser. All optical filters are listed together with the fluorochromes used in this manuscript.

Titrations

The panel was developed based on cell surface molecules of interest for NK cell characterization. Different priority levels were assigned regarding the importance of inclusion in the final panel, as well as the availability of fluorochrome conjugates (2). Before assessing each new iteration of the panel, all reagents were titrated by at least two-fold dilution series. The **Online Figure 1** depicts the titrations of the antibodies used in the optimized panel.

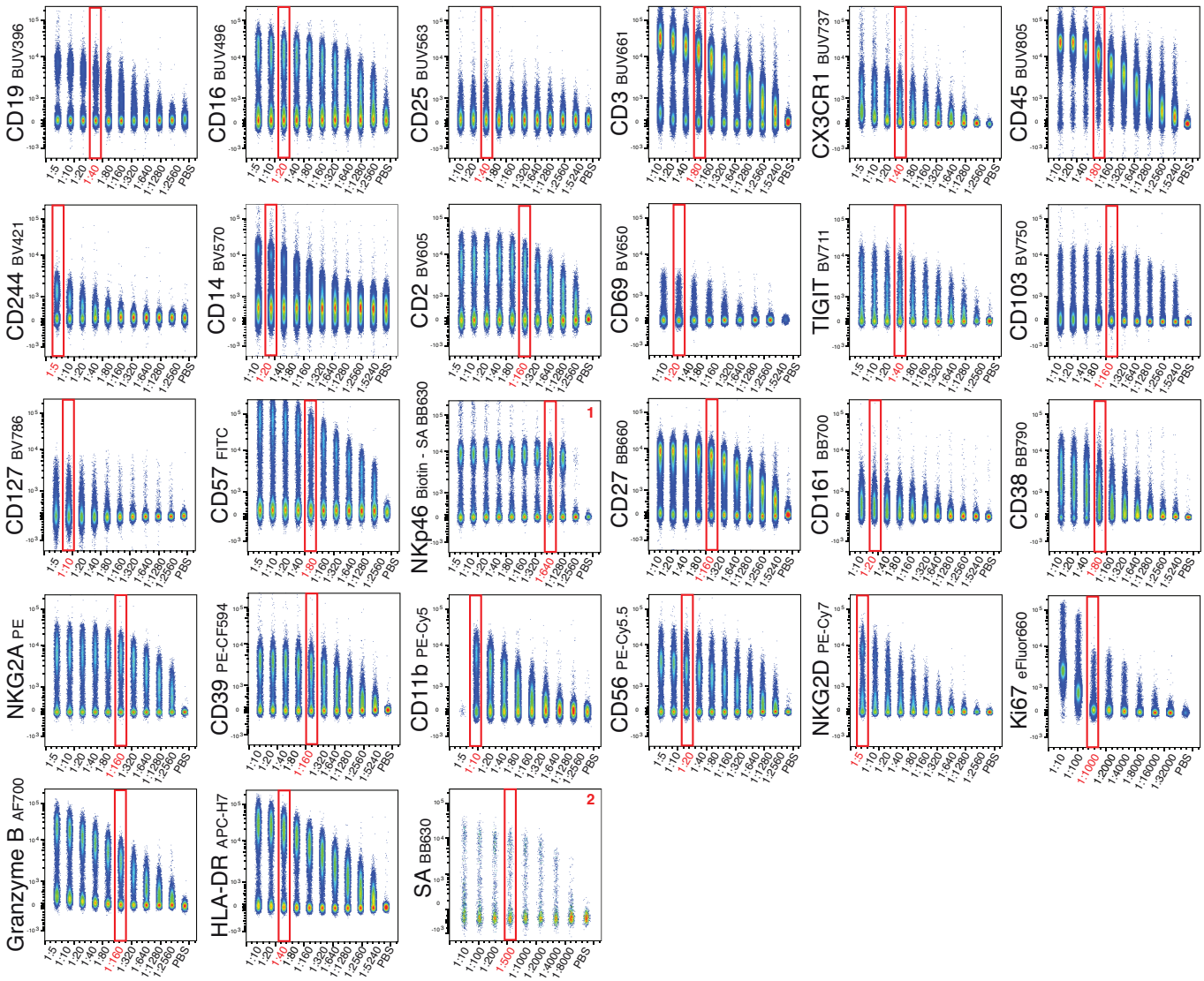

Online Figure 1: Titrations of the antibodies used in the optimized panel

Reagents were titrated using cryopreserved PBMCs from healthy donors, by performing at least 8 2-fold dilution steps (specific dilutions are indicated below each plot). Individual .fcs files were concatenated in order to visualize all titrations in one single plot. Decreasing antibody-concentrations are arranged along the x axis. "PBS" is referring to an unstained sample. The optimal titers used for a given antibody was mostly chosen based on the concentration leading to the higher Stain Index (SI) ratio. SI was calculated, using FlowJo 10.6.0, as followed: (median^{+} - median^{-}) / ((percentile 84 of the median of the negative population – median^{-})/0.995). For some antibodies without a clearly defined positive population, the best titer was chosen based on the near maximal signal without increasing background signal. Finally, for some marker (primarily lineage markers), we did not choose the titer with the highest SI in order to safe reagent as separation was deemed sufficient and no saturating titer was required. Titers that were selected in this OMIP are highlighted in red. Titers are given as dilution factors for a final staining volume of 50 µL for 2-5 x 10^6 cells. (1. Titration of the NKp46 Biotin. SA BB630 was used at 1:500. 2. Titration of the SA BB630. NKp46 Biotin was used at 1:640).

Panel design guided by spreading error (SE)

Spreading error is the single most relevant contributor to loss of resolution and this panel was designed using a spill-over spreading error matrix (SSM) to predict problematic combination of fluorochromes. The SSM generated provides an overview, for a specific instrument and a specific panel, of the relative contribution of any fluorophore to generate spillover spreading error in secondary detectors as well as the relative loss of resolution in any secondary detector due to spillover spreading error collected from all other fluorophores (2-4). Ultimately, the SSM helps designing a multicolor panel as problematic pairs of fluorochromes can be anticipated with a high numerical value. Here, we identified the following problematic pairs, both by their high value in the SSM as well as visual inspection of the spreading error on two-dimensional plots (data not shown), that could predict a loss of resolution in secondary detectors due to the:

- Spreading error of the BB 630 fluorochrome into the G610 and V610 detectors
- Spreading error of the BB 790 fluorochrome into the V780 detector
- Spreading error of the PE-CF594 fluorochrome into the B610 detector
- Spreading error of the PE-Cy5.5 fluorochrome in the B710 detector
- Spreading error of the BUV661 fluorochrome in the R660 detector
- Spreading error of the BV650 fluorochrome in the R660 and U660 detectors

Of note, the final SSM was generated with the antibodies used in the optimized panel (**Online Table 2**), and is displayed in the **Online Figure 2.**

Specificity	Clone	Fluorochrome	Vendor	Catalog number	Titration
Dead cells	UV	Blue	Invitrogen	L34962	1:500
CD45	HI30	BUV805	BD	564914	1:80
CD14	M5E2	BV570	BioLegend	301832	1:20
CD19	SJ250-C1	BUV395	BD	563549	1:40
CD3	UCHT1	BUV661	BD	565065	1:80
CD127	HIL-7R-M21	BV786	BD	563324	1:10
HLA-DR	G46.6	APC-H7	BD	641393	1:40
CD16	3G8	BUV496	BD	564653	1:40
NKp46	9E2	Biotin	BioLegend	331906	1:640
Streptavidin		BB630	BD custom antibody	624294	1:500
NKG2D	1D11	PE-Cy7	BD	562365	1:5
CD244	2-69	BV421	BD	565750	1:5
CD2	RPA-2.10	BV605	BioLegend	300224	1:160
NKG2A	REA110	PE	Miltenyi	130-113-566	1:160
CD161	DX12	BB700	BD	745791	1:20
TIGIT	741182	BV711	BD	747839	1:80
CD69	FN50	BV650	BioLegend	310933	1:20
CD39	TU66	PE-CF594	BD	563678	1:160
CD57	NK-1	FITC	BD	555619	1:80
CD27	M-T271	BB660	BD custom antibody	624295	1:160
CD11b	ICRF44	PE-Cy5	BD	555389	1:10
CD38	HIT2	BB-790-P	BD custom antibody	624896	1:80
CX3CR1	2A9-1	BUV737	BD	749355	1:40
CD103	Ber-ACT8	BV750	BD	747099	1:160
Ki67	Sola15	eFluor660	eBiosciences	50-5698-80	1:1000
GranzymeB	QA16A2	AF700	BioLegend	372222	1:160
CD25	2A3	BUV563	BD	565699	1:40
CD56	CMSSB	PECy5.5	ThermoFisher	35-0567-41	1:20

Online Table 2: Antibodies used in the optimized panel

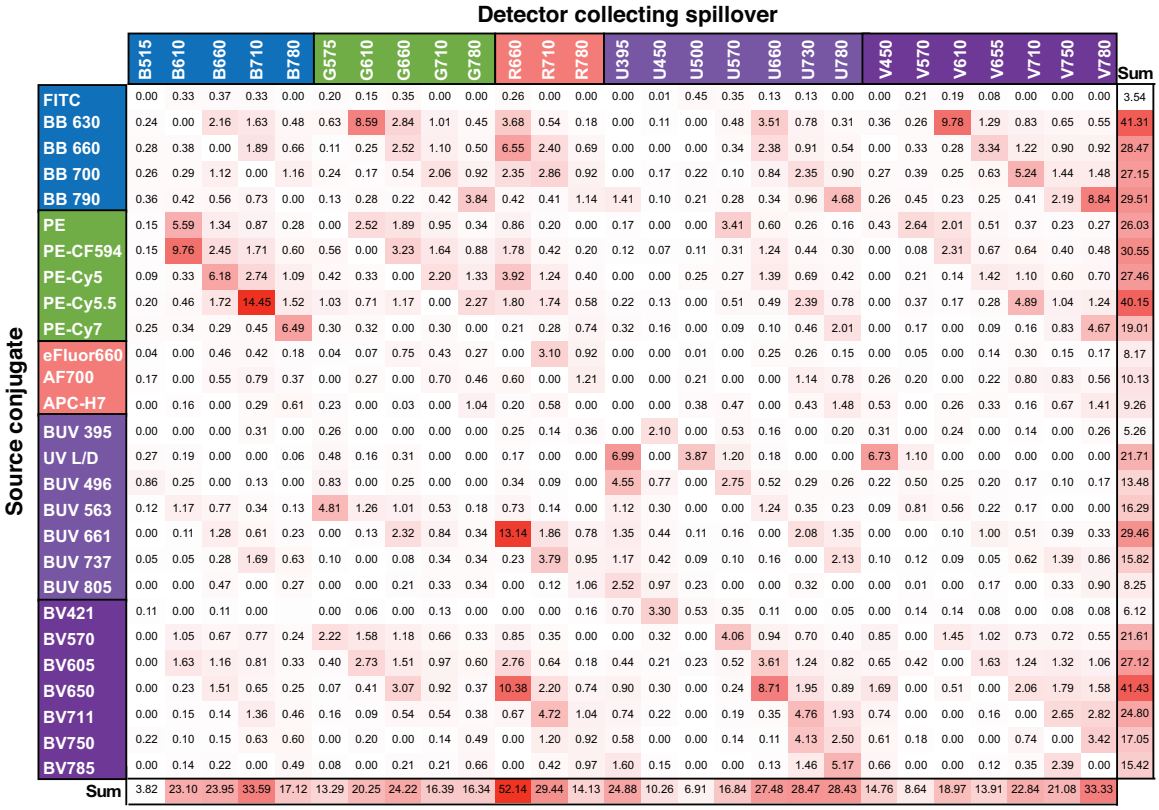

Online Figure 2: Spillover Spreading Matrix

The spillover spreading matrix (SSM) was calculated using FlowJo 10.6.0 with the single-stained controls of the compensation beads using the reagents from the optimized panel. Spreading error values are highlighted with a color gradient with white being a low spreading error and red a high spreading error.

Establishment of the first iteration

Some of the antibodies included in this panel have been successfully tested in OMIP-44 such as: CD3 BUV661, CD16 BUV496, CD56 BUV563, CD45 BUV805, CD19 PE-Cy5.5, CX3CR1 PE-Cy7 and HLA-DR APC-H7 (5). Based on their preexistence and availability in the laboratory, these reagents were included in the first iteration of the panel and optimized if necessary (**Online Table 3**). The optimization process was initially performed on cryopreserved PBMC samples from healthy donors. Starting at the 3rd iteration, each panel was also tested on human healthy or tumor tissues.

	Iteration 1	Iteration 2	Iteration 3	Iteration 4	Iteration 5	Iteration 6	OPTMIZED PANEL
BUV395	CD4 (RPA-T4)	CD4 (RPA-T4)	CD4 (RPA-T4)	**CD4 (RPA-T4)**	CD25 (2A3)	CD19 (SJ25-C1)	CD19 (SJ25-C1)
UV L/D	L/D	L/D	L/D	L/D	L/D	L/D	L/D
BUV496	CD16 (3G8)	CD16 (3G8)	CD16 (3G8)	CD16 (3G8)	CD16 (3G8)	CD16 (3G8)	CD16 (3G8)
BUV563	CD56 (NCAM16.2)	CD56 (NCAM16.2)	CD56 (NCAM16.2)	CD56 (NCAM16.2)	CD56 (NCAM16.2)	CD25 (2A3)	CD25 (2A3)
BUV661	CD3 (UCHT1)	CD3 (UCHT1)	CD3 (UCHT1)	CD3 (UCHT1)	CD3 (UCHT1)	CD3 (UCHT1)	CD3 (UCHT1)
BUV737			CX3CR1 (2A9-1)	CX3CR1 (2A9-1)	CX3CR1 (2A9-1)	CX3CR1 (2A9-1)	CX3CR1 (2A9-1)
BUV805	CD45(HI30)	CD45(HI30)	CD45(HI30)	CD45(HI30)	CD45(HI30)	CD45(HI30)	CD45(HI30)
BV421	CD122 (Mik-b3)	CD122 (Mik-b3)	CD122 (Mik-b3)	**CD122 (Mik-b3)**	CD244 (2-69)	CD244 BV421 (2-69)	CD244 BV421 (2-69)
BV480	CD161 (DX12)	CD161 (DX12)					
BV570		CD14 (M5E2) BV570	CD14 (M5E2)	CD14 (M5E2)	CD14 (M5E2)	CD14 (M5E2)	CD14 (M5E2)
BV605	NKG2A (131411)	NKG2A (131411)	NKG2A (131411)	NKp46 BV605	CD2 (RPA-2.10)	CD2 (RPA-2.10)	CD2 (RPA-2.10)
BV650	Tim3 (7D3)	Tim3 (7D3)	Tim3 (7D3)	Tim3 (7D3)	Tim3 (7D3)	**Tim3 (7D3)**	CD69 (FN50)
BV711	NKp46 (9E2)	NKp46 (9E2)	TIGIT (741182)	TIGIT (741182)	TIGIT (741182)	TIGIT (741182)	TIGIT (741182)
BV750	CD103 (Ber-ACT8)	CD103 (Ber-ACT8)	CD103 (Ber-ACT8)	CD103 (Ber-ACT8)	CD103 (Ber-ACT8)	CD103 (Ber-ACT8)	CD103 (Ber-ACT8)
BV785	CD127 (HIL-7R-M21)	CD127 (HIL-7R-M21)	CD127 (HIL-7R-M21)	CD127 (HIL-7R-M21)	CD127 (HIL-7R-M21)	CD127 (HIL-7R-M21)	CD127 (HIL-7R-M21)
BB515	CD57 (NK-1)	CD57 (NK-1)	CD57 (NK-1)	CD57 (NK-1)	CD57 (NK-1) FITC	CD57 (NK-1) FITC	CD57 (NK-1) FITC
BB630			NKp46 (9E2)	NKG2A (REA110)	NKp46 (9E2)	NKp46 (9E2)	NKp46 (9E2)
BB660	PD-1 (MIH4)		CD27 (M-T271)	CD27 (M-T271)	CD27 (M-T271)	CD27 (M-T271)	CD27 (M-T271)
BB700	NKG2D (1D11)	NKG2D (1D11)	CD161 (DX12)	CD161 (DX12)	CD161 (DX12)	CD161 (DX12)	CD161 (DX12)
BB790	TIGIT (741182)	TIGIT (741182)	CD38 (HIT2)	CD38 (HIT2)	CD38 (HIT2)	CD38 (HIT2)	CD38 (HIT2)
PE	CD244 (2-69)	CD244 (2-69)	CD244 (2-69)	CD244 (2-69)	NKG2A (REA110)	NKG2A (REA110)	NKG2A (REA110)
PE-CF594		PD-1 (EH12)	PD-1 (EH12)	PD-1 (EH12)	PD-1 (EH12)	**PD-1 (EH12)**	CD39 (TU66)
PE-Cy5	CD11b (ICRF44)	CD11b (ICRF44)	CD11b (ICRF44)	CD11b (ICRF44)	CD11b (ICRF44)	CD11b (ICRF44)	CD11b (ICRF44)
PE-Cy5.5	CD19 (SJ25-C1)	CD19 (SJ25-C1)	CD19 (SJ25-C1)	CD19 (SJ25-C1)	CD19 (SJ25-C1)	CD56 (CMSSB)	CD56 (CMSSB)
	CD14 (TuK4)						
PE-Cy7	CX3CR1 (2A9-1)	CX3CR1 (2A9-1)	NKG2D (1D11)	NKG2D (1D11)	NKG2D (1D11) PE-Cy7	NKG2D (1D11)	NKG2D (1D11)
AF647	Ki67 (Sola15)	Ki67 (Sola15)	Ki67 (Sola15)	Ki67 (Sola15)	Ki67 (Sola15)	Ki67 (Sola15)	Ki67 (Sola15)
AF700	GranzymeB (GB11)	GranzymeB (GB11)	GranzymeB (GB11)	GranzymeB (GB11)	GranzymeB (QA16A2)	GranzymeB (QA16A2)	GranzymeB (QA16A2)
APC-H7	HLA-DR (G46.6)	HLA-DR (G46.6)	HLA-DR (G46.6)	HLA-DR (G46.6)	HLA-DR (G46.6)	HLA-DR (G46.6)	HLA-DR (G46.6)

Antibody	Orange bold writing: antibodies that have to be used with another fluorochrome / clone for the next iteration
Antibody	Red bold writing: antibodies that are going to be removed for the next iteration
Antibody	Blue filling: antibodies that have been added compare to the previous iteration
Antibody	Orange filling: antibodies which have changed fluorochrome or clone compare to the previous iteration

Online Table 3*: *Toward the 27-color optimized panel

This table outlines the evolution of the panel. Each column represents one tested panel. Orange bold writing indicates that the antibodies were used with a different fluorochrome or clone in the next iteration. Red bold writing indicates that the antibodies were removed in the next iteration. Orange filling highlights antibodies, which were changed to different fluorochrome or clone compared to the previous iteration. Blue filling highlights antibodies that have been added compared to the previous iteration.

For the first iteration, a “double dump” channel was assigned to the PE-Cy5.5 channel in order to discard at the same time B cells (CD19) and monocytes (CD14). However, in order to be able to enumerate B cells and monocytes separately, for the rest of the panel development, each marker was assigned to a separate fluorochrome. Tested antibodies that were excluded after each new iteration are listed in the **Online Table 4** along with the explanation for their removal.

Specificity	Flurorochrome	Clone	Reason
CD14	PE-Cy5.5	TuK4	"Double dump" channel prevented the enumeration of B cells and monocytes separately. CD14 was switched to BV570
PD-1	BB660	MIH4	Not great signal linked to the spreading error from CD14 and CD19 PE-Cy5.5 into the B660 detector. PD-1 was used with a different clone and switched to PE-CF594
CD161	BV570	BV480	Great signal but, to free up V510 detector. CD161 was switched to BB660
NKG2D	BB700	1D11	NKG2D BB700 induced a lot of spreading error in different detectors as G575, G660, R660, R710 and U660. But most of all, lot of spreading error in the B710 detector which resulted in a bad signal for NKp46 BV711. NKG2D was switched to PE-Cy7
NKp46	BV711	9E2	Bad separation between positive and negative cells, lot of spreading error coming from NKG2D BB700 and CD11b PE-Cy5. Moreover, NKp46 BV711 induced a lot of spreading error in the B710, G710 and R710 detectors. NKp46 was switched to BB630 (using a biotin conjugated antibody)
CX3CR1	PE-Cy7	2A9-1	Great separation but induced a lot of spreading error in the B780 detector. CX3CR1 was switched to BUV737
TIGIT	BB790	741182	Great signal but TIGIT was switched to BV711 in order to use a more frequently used marker coupled to the BB790 fluorochrome
NKG2A	BV605	131411	Bad separation between positive and negative cells and spreading error coming from NKp46 Biotin SA BB630 in the V610 detector. NKG2A was used with a different clone (REA110) and moved to BB630 (using a biotin conjugated antibody)
NKG2A	Biotin - SA BB630	REA110	Great separation between positive and negative cells. However, NKp46 had the highest priority and had a better separation using this Biotin - SA BB630 combination. NKG2A was moved to PE.
NKp46	BV605	9E2	Separation less optimal compared to the biotin - SA BB630 combination. NKp46 was moved again to BB630 (using a biotin conjugated antibody)
CD4	BUV395	RPA-T4	Great separation but not really informative for this panel. CD4 was definitively removed
CD122	BV421	Mik-b3	Great separation but not really informative for this panel. In the different tested samples, all NK cells express CD122. CD122 was definitively removed
CD244	PE	2-69	Great separation. However, as NKG2A was used with the PE fluorochrome, CD244 was switched to BV421 that gave a comparable brightness.
Granzyme B	AF700	GB11	Great separation, but to obtain a consistent staining between samples, Granzyme B was used with a different clone
CD25	BUV395	2A3	Spreading error from CD16 BUV496 in the U395 detector prevented studying the expression of CD25 among NK cells. CD25 was switched to BUV563.
CD56	BUV563	NCAM16.2	Really great separation but not really useful to develop the immunophenotyping of NK cells in tissues. As CD25 was moved to BUV563, CD56 was moved to PE-Cy5.5
CD19	PE-Cy5.5	SJ25-C1	Really great separation but as CD56 was moved to PE-Cy5.5, CD19 was switched to BUV395
Tim3	BV650	7D3	Great separation to observe Tim3 expression among circulating NK cells. However, Tim3 was collagenase-sensitive which prevented to clearly study the differential expression in tissues. Tim3 was definitively removed
PD-1	PE-CF594	EH12	Great separation. However, we did not observe PD-1 expression by NK cells. PD-1 was definitively removed

Online Table 4: Tested and excluded reagents

This table recapitulates the motives for excluding a given antibody during the panel development

2. Unambiguous identification of NK cells as a crucial goal for the success of this panel

One of the main goals for this panel was to find a strategy that would allow for unambiguous NK cell characterization of both human peripheral blood NK cells and NK cells in tumor tissue. After we observed consistently that CD56 expression was impaired by collagenase

digestion in tumor tissue samples (**Figure 1 main manuscript**), it became clear that another marker will be required to discriminate NK cells. NKp46, a member of the Natural Cytotoxicity Receptor (NCR) family (also named NCR1 or CD335), was described as being expressed by all NK cells and even a good candidate to discriminate NK cells across species (6,7). Furthermore, as shown in the **Online Figure 3**, we believe that our new NKp46-gating strategy enabled to capture all known NK cell subsets.

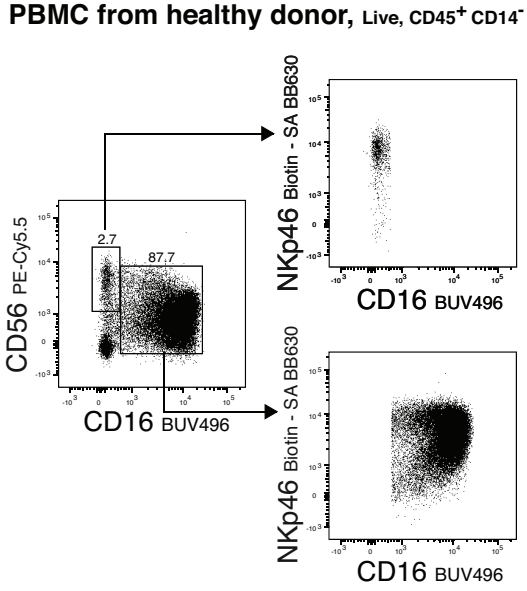

Online Figure 3: NKp46 vs CD16 distribution among the CD56^{bright} CD16^{-} and CD56^{dim} CD16^{+} NK cell subsets.
Cryopreserved PBMCs from one healthy donor were stained with the optimized panel and dot plots are showing the distribution of NKp46 vs CD16 in comparison with the known NK cell subsets.

We used clone 9E2 as it has already been shown to efficiently stain NK cells from both human peripheral blood and different murine organs (8,9). Three different fluorochromes for NKp46 were tested: BV711, BV605, and Biotin combined with Streptavidin (SA) BB630. NKp46 BV711 gave a poor signal of the positive population. Moreover, in the first two iterations of the panel development, the V710 detector received a lot of spreading error from both NKG2D BB700

and CD11b PE-Cy5 leading to an unsatisfactory signal. NKp46 BV605 gave a better signal for the positive population but the separation between the positive and the negative population was less optimal compared to the NKp46 Biotin. The titrations for these three antibodies are shown in **Online Figure 4** along with the bivariate dot plots showing the relative density population of NK cells along the two parameters CD16 and the different NKp46 tested. These last dot plots indicate that NKp46 Biotin – SA BB630 is a perfect fit for the requirement of this panel. Importantly, we tested both the direct conjugate NKp46 BB630 and the combination NKp46 Biotin – SA BB630 and chose to keep the combination NKp46 Biotin – SA BB630 as it had a superior resolution (data not shown).

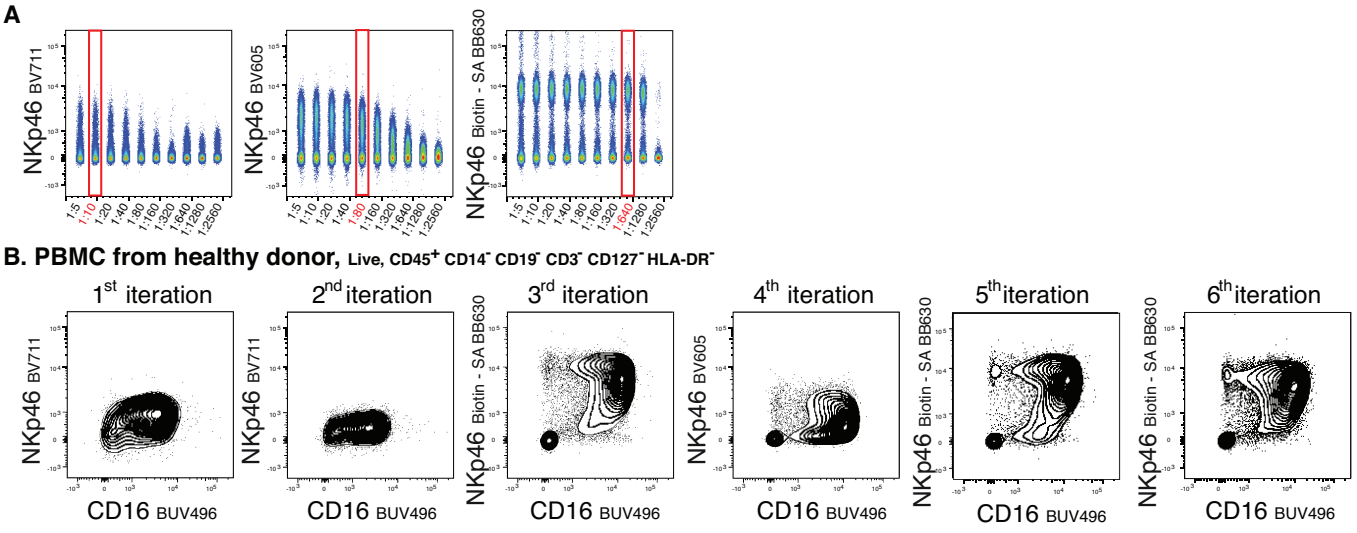

Online Figure 4: Different tested NKp46.

A. *Dot plots representing the titration of NKp46 with different fluorochromes. Titrations were assessed as described in Online Figure 1* ***B.*** *Cryopreserved PBMCs from one healthy donor were stained with the different panels (described in Online Table 3). Dot plots represent the NK cell populations along the two parameters CD16 and NKp46 for each designed iteration.*

3. Definition of the markers of interest to be included in this panel

After defining NKp46 as the main marker used to identify NK cells in tissues, the second priority was given to the inclusion of targets to assess the functional potential of all NK cell populations. Importantly, in the following description each marker of the panel is assigned to one function. However, one should keep in mind that depending on the environment, these included markers could possess different functions and are not restricted to the one described in the following sections. However, together, these markers should help in identifying changes within the NK cell compartment.

Activating and inhibitory receptors

First, NK cell activation is regulated by a broad family of activating and inhibitory receptors. NK cells have to integrate signals from these multiple receptors in order to sense their environment and respond appropriately.

Activating receptors:

NKp46 was already included as a critical marker to discriminate NK cells.

CD244 (2B4), a member of the Signaling Lymphocyte Activation Molecule (SLAM) family, was included as it has been shown to be a potential target for immunotherapy. Indeed, CD244's possible dual functionality being both activating under normal conditions or inhibitory in the context of the tumor microenvironment (10) is intriguing. CD244 was first tested with clone 2-

69, coupled to the PE fluorochrome, which gave a great separation between positive and negative population. However, during the panel development we have moved the NKG2A inhibitory receptor to the PE fluorochrome, which has led us to use CD244 with another fluorochrome. As CD244 is dimly expressed, it required a fluorochrome with a comparable brightness compared to PE. As, BV421 is a typically bright fluorophore with a comparable brightness compared to the PE fluorochrome, we have moved CD244 to this fluorochrome. Moreover, it was a great option as it did not receive a lot of spreading error from other fluorochromes. Finally, it was an available option as we had decided to remove CD122-BV421 from the panel.

CD2, a cell adhesion molecule, was also included as another activating receptor. CD2 has been shown to be relevant for the co-activation of NK cells as well as the formation of a memory subset (11,12). The RPA-2.10 clone was used as it has been successfully tested in a previously published OMIP (13). When we titrated CD2, we noticed that it was highly expressed by NK cells. We considered that this high CD2 signal could be used with a detector receiving spreading error. Given the known spreading error from the BB630 fluorochrome into the V610 detector (see below for NKG2A), we decided to insert CD2 coupled to BV605 which resulted in a great signal with minimal spill-over or spread issues.

Inhibitory receptors:

The inhibitory receptors include the C-type lectin family (NKG2A, CD161) and the killer-cell immunoglobulin-like receptor family (KIR). NKG2A and CD161 were both included in this panel. In addition to its role as an inhibitory receptor, NKG2A has been proposed as a biomarker

to distinguish a continuous differentiation process of $CD56^{dim}$ NK cells, from a $NKG2A^{+}KIR^{-}CD57^{-}$ to a $NKG2A^{-}KIR^{+}CD57^{+}$ $CD56^{dim}$ NK cell phenotype (14), and is, as such, an interesting marker to include in this panel. NKG2A was first tested with the clone 131411 coupled to the BV605 fluorochrome. As NKG2A is highly expressed by NK cells (15), spreading error in the V610 detector from the BB630 fluorochrome should not be an issue. However, we did not obtain optimal staining of the positive population with the 131411 clone. Moreover, as anticipated, a spreading error from the BB630 fluorochrome into the V610 detector was observed which led us to change the NKG2A clone (Miltenyi clone REA110) and to move this antibody to the B610 channel using a biotinylated antibody linked to the SA BB630. This is the reason why NKp46 was moved to the BV605 fluorochrome in the 4^{th} iteration. This setting led to a great staining of NKG2A. However, the amplification of the signal of the NKp46 BV605 was less convincing compare to the Biotin - SA BB630 combination tested in the third iteration. As it appeared that NKG2A staining issue was more related to the clone than the fluorochrome, NKp46 was moved back to the B610 channel. NKG2A was used coupled to the PE fluorochrome in the 5^{th} iteration and yielded a good result for the staining of the positive fraction as well as the separation between the positive and the negative populations.

CD161 inhibitory receptor expression has been linked to NK cell cytokine-responsiveness and blocking the interaction with its LLT1 ligand has been shown to increase NK cell cytotoxicity against breast cancer cells (16), which make this marker a good candidate to include in our panel. CD161 clone DX12 BV480 was first tested but was then moved to the BB700 fluorochrome, which enabled to free up V510 for autofluorescence exclusion.

We then tested antibodies against proteins with inhibitory properties such as TIGIT (17), PD-1 and Tim3 (18). TIGIT BB790 (clone 741182) was first tested and resulted in a good staining. However, in order to be able to use CD38 BB790, more frequently used in the laboratory, TIGIT was moved to the BV711 fluorochrome.

Importantly, the two other inhibitory checkpoints tested in this panel (Tim3 and PD-1) were eventually removed from the optimized panel. Detection of Tim3 expression was sensitive to collagenase treatment, and, in line with a recent publication (19), we also did not observe PD-1 expression on NK cells isolated from different tumor samples. We considered that the lack of detection could also be specific for the anti-PD-1 clone used in the study. We tested two different clones (MIH4 and EH12) with the same negative result. A recent study reported that only the PD.1.3.1.3 clone was able to efficiently separate the PD-1^{+} from the PD-1^{-} NK cells (20) . However, this specific clone is not widely available yet with a limited choice of fluorochromes. This has led us to remove this antibody from the optimized panel.

Maturation and activation

Since immune activation, maturation and differentiation are important aspects in tumor immunology, some markers used to delineate these NK cell states were added to this panel.

Maturation

Since they have been shown to define NK cell maturation in different contexts, CD11b, CD27 and CD57 antibodies were included in this panel (7,14,21). Because of their availability in the laboratory, CD57 clone NK-1 coupled to the FITC fluorochrome, CD11b clone IRCF44 coupled

to the PE-Cy5 fluorochrome and CD27 clone M-T271 coupled to the BB660 fluorochrome, were tested in the first panel. Each of them demonstrated a clear separation of positive and negative populations within $CD45^+$ cells and were kept the same along process optimization. CD27 expression among $lineage^-$ NK cells was low, however, as variation in its expression has been observed between tissue samples, CD27 was kept in the panel and could be useful for in-depth definition of NK cell subsets.

Activation

First, CD56 was kept in the panel as a phenotypic marker of activation (22). Importantly, although detection of CD56 expression was shown to be decreased by collagenase treatment, the comparison of its expression between two types of tissues could still be informative. Moreover, as CD56 possesses a major role in distinguishing NK cell subsets within the blood, keeping this marker would still allow for subsetting NK cells within the peripheral blood using the common strategy of $CD56^{bright}$ $CD16^{neg}$ or $CD56^{dim}$ $CD16^+$ cells to ensure that new studies can be compared with previous studies.

CD56 clone NCAM-16.2 was first tested coupled to the BUV563 fluorochrome and yielded an excellent separation of expression. However, during the optimization process, CD56 was moved to the PECy5.5 fluorochrome, which still allowed for a clear separation of the negative and positive populations. This modification was due to the inclusion, in the 5^{th} iteration, of CD25 BUV395, as another marker of activation (23-26). In the 4^{th} iteration, a spreading error from CD16 BUV496 in the U395 detector was observed obscuring the expression of CD25. To fix this issue, CD25 was moved to the U570 detector, with the BUV563 fluorochrome, that received moderate

spreading error from other fluorochromes and which resulted in well separated CD25 populations. Because of this change CD56 was moved to the PE-Cy5.5 channel.

CD38 was included as a marker of NK cell activation. A recent study linked CD38 expression to NK cell cytotoxic activity against tumor cells (27) highlighting the importance of including this marker.

Finally, granzyme B and Ki67 were also included in this panel as classical markers of cytotoxic potential and the ability to proliferate, respectively. Granzyme B coupled to AF700 and Ki67 to eFluor660 were first tested and were kept during panel development. However, we made one modification for granzyme B and switched from the GB11 clone to the QA16A2 clone. The main reason was the sporadic (and seemingly random) shift of the negative population from the blood to a higher staining intensity compared to the negative population of the tumor. In OMIP60, authors have compared the two clones GB11 and QA16A2 and reported a similar staining efficiency (28). Since clone QA16A2 was also available coupled to AF700, we used it from here on for our panel development. However, random shifts of the negative population from the blood to a higher staining intensity were still observed with clone QA16A2.

Migration and residency

Lastly, as the goal of this OMIP is to define NK cell populations in human tumor tissues and peripheral blood, migration and residency markers were included in this panel. CD103 and CD69 are classical markers of tissue-resident memory T cells (29). Since they have also been shown to be expressed by tissue-infiltrating NK cells (30-32), they were both included in this panel. CX3CR1 was also included as its expression at the surface of NK cells is modulated in tumor

tissues (33,34). CX3CR1 was first tested coupled to the PE-Cy7 fluorochrome, which induced a lot of spreading error in the B780 detector. As we wanted to include CD38 BB790 that is not highly expressed by NK cells, we needed to reduce this spreading error, and this is the reason why CX3CR1 was moved to the BUV737 channel. With this fluorochrome, it displayed a clear separation between positive and negative population.

CD39 was also included as a tissue residency marker. CD39 could be a marker of chronic antigen stimulation, which could be the case within a tumor tissue. CD39 is of interest as a therapeutic target to prevent adenosine-triggered immune-suppressive effect (35). CD39 was used coupled to the PE-CF594 where a moderate spreading error from the NKp46 Biotin – BB630 into the G610 detector was detected. We used $CD3^+$ T cells that expressed CD39 (35), to set the threshold of CD39 positivity (**Online Figure 5**). Given that we could identify cells with high expression of CD39 and given the lack of a better alternative approach, we settled with this combination.

As a caveat, this combination would inevitably prevent us to study a possible intermediate expression of CD39 by NK cells. However, to date, there are no publications regarding the expression patterns of CD39 on human NK cells. In our analyzed tissues, we were able to see increased expression of CD39 by infiltrating NK cells, so we decided to keep CD39 PE-CF594 (**Figure 1 main manuscript**).

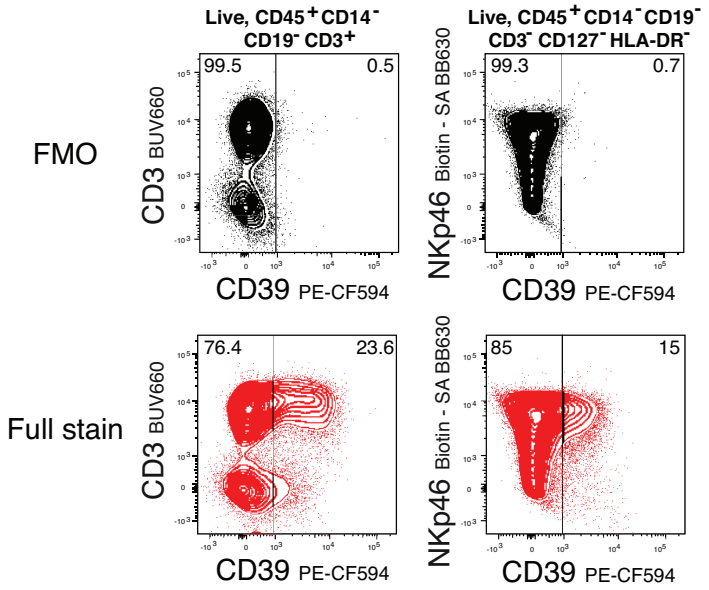

Online Figure 5: Threshold of CD39 positivity

Single FMO for the CD39 marker was performed on one tumor tissue. Upper black dot plots represent the FMO expression and lower red dot plots represent the corresponding full staining for the lineage-gated CD3⁺ T cell population (left plots), and NK cell population (right plots). Numbers indicate the percentage of cells in the indicated gate.

Other excluded reagents

Other antibodies were also tested during the panel development process but were ultimately excluded from the final panel. CD122 was tested in the first panels but a constitutive expression across all NK cells was observed, which has led to its exclusion as it would not be informative to address NK cell activation. CD4 was also tested in the first panels to distinguish T cell subsets. However, as other markers to study NK cells were included, CD4 was finally removed from the panel. And lastly, as already mentioned, Tim3 and PD-1 were also investigated, but were removed due to impaired expression after collagenase-treatment, and absence of expression in the different tested samples for PD-1, respectively.

4. Final remarks for this panel development:

Collagenase treatment

Because this staining panel was designed to elucidate NK cell phenotype within tumor tissues and peripheral blood, one of the challenges was to verify that the expression of the markers used in the different iterations of the panel was not impaired during tissue dissociation. As shown in the **Online Figure 6**, the expression of each of the used markers in the optimized panel is not impaired by collagenase digestion.

A. PBMC from healthy donor, Live, CD45$^+$ CD14$^-$ CD19$^-$ CD3$^-$ CD127$^-$ HLA-DR$^-$

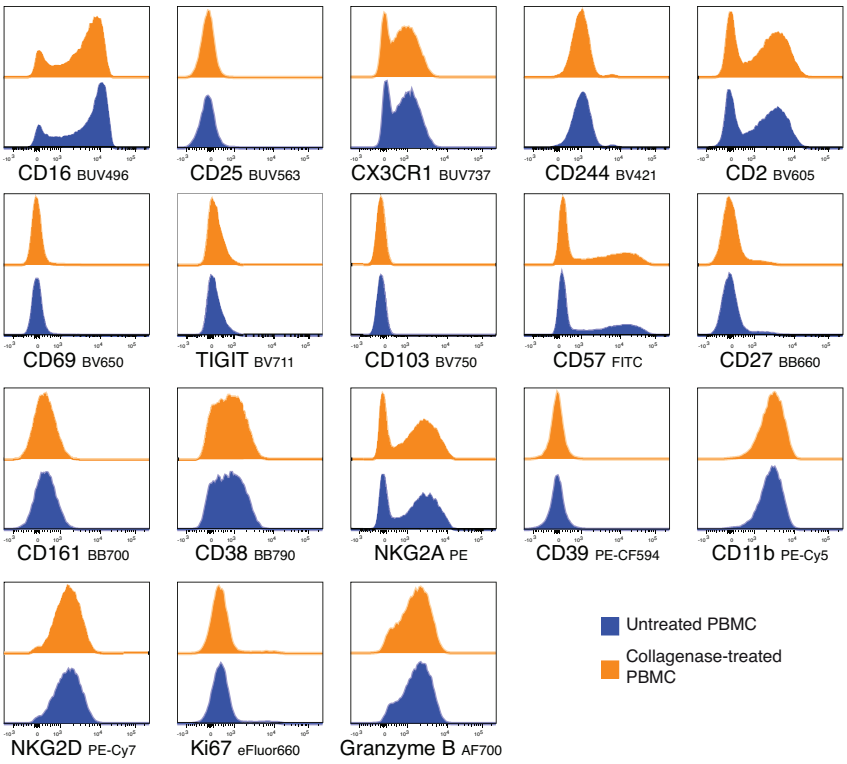

B. PBMC from healthy donor, Live, CD45$^+$ CD14$^-$ CD19$^-$ CD3$^+$

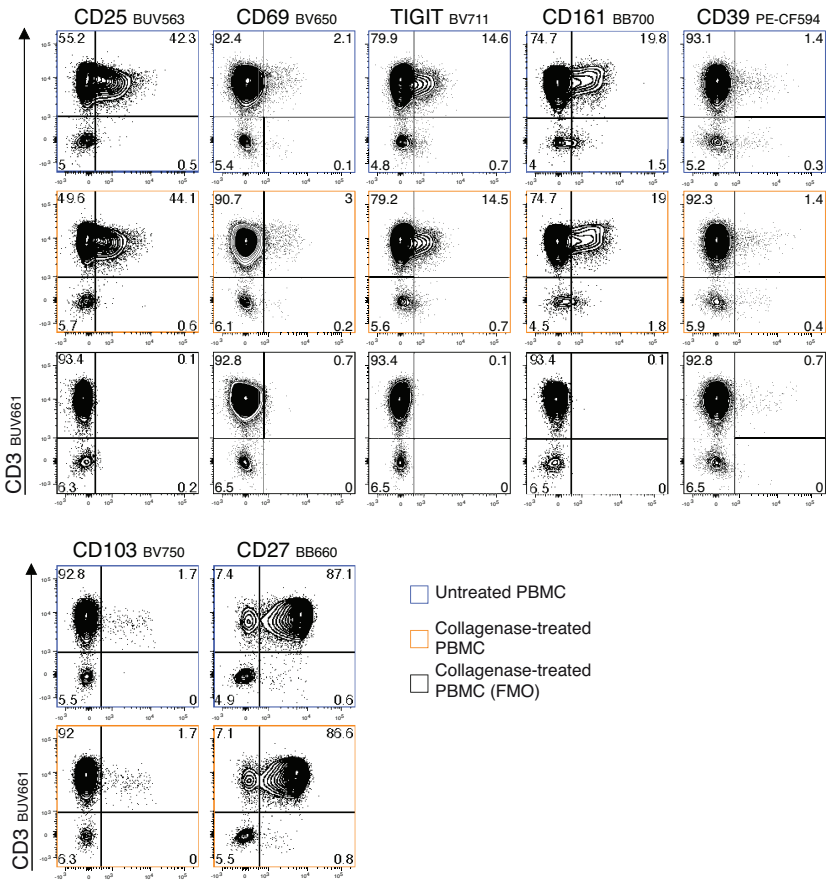

359

Online Figure 6: Collagenase digestion did not alter other markers.

*PBMCs from one healthy donor were digested with type II collagenase. Histograms and dot plots are representing the expression of the markers used to define NK cell population in respectively the **A.** Lineage-gated NKp46$^+$ cells and **B.** Lineage-gated CD3$^+$ T cells. Numbers indicate the percentage of cells in the indicated gate.*

Fluorescence Minus One controls

During panel development, Fluorescence Minus One (FMO) controls were used to exclude any unforeseen issues for all markers expressed at low levels. For the optimized panel, FMO controls should be used to determine gate placement of CD39, CD25, TIGIT, CD161 and CD56. If this panel is only used for NK cell characterization in the blood, CD69 FMO should also be added. Indeed, while the positive and negative population of CD69-expressing NK cells are clearly defined within infiltrated NK cells, the gate placement could be harder to set up in order to distinguish the CD69$^+$ from the CD69$^-$ population within circulating NK cells (**Online Figure 7**).

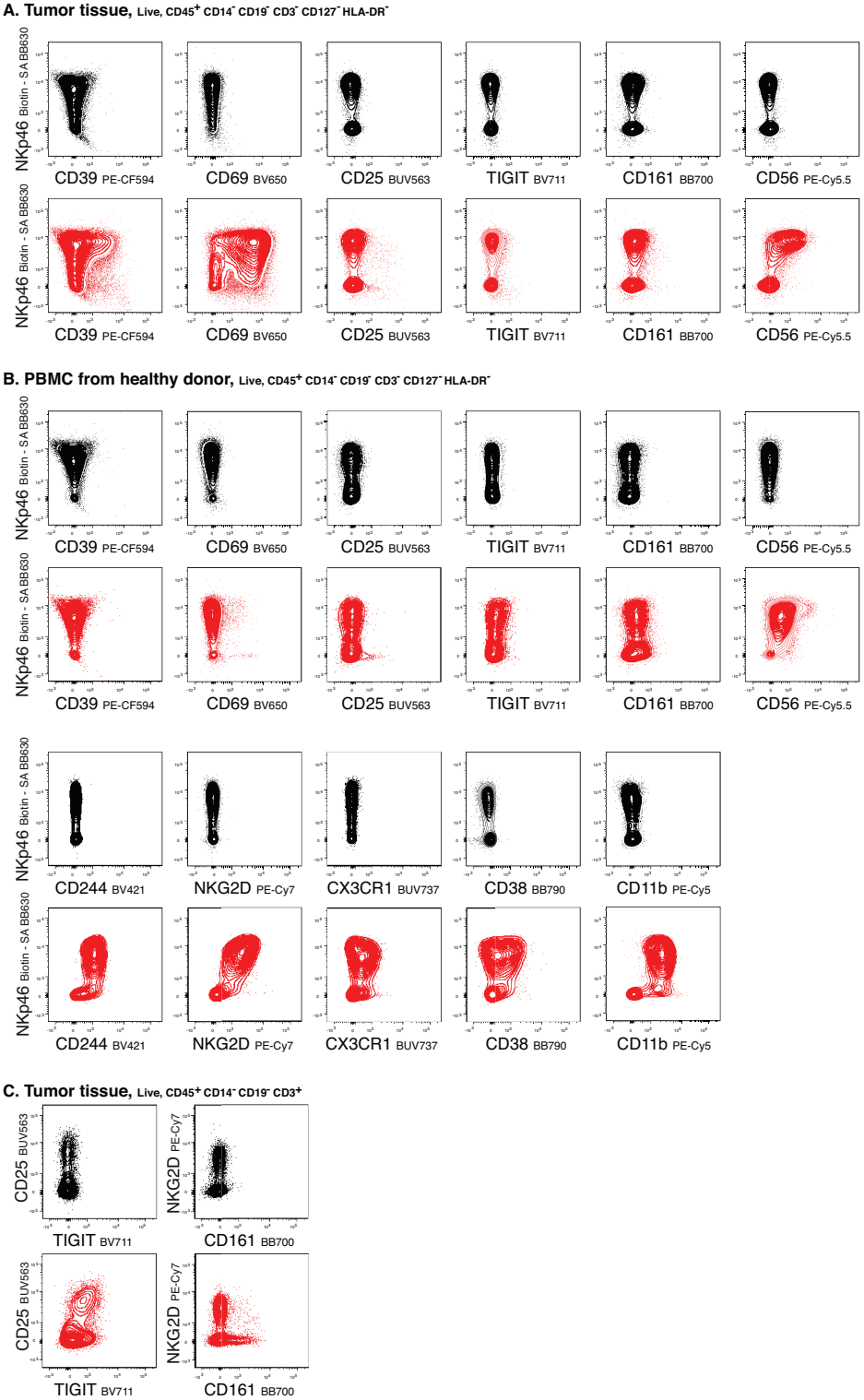

Online Figure 7: FMO from both blood and tissue.

*Single FMO controls were performed on **A. C.** two different tumor tissues **B.** PBMC from one healthy donor. In **A., B. and C.,** upper black dot plots represent the FMO expression and lower red dot plots represent the corresponding full staining for the lineage-gated **A. B.** NK cell population, and **C.** $CD3^+$ T cell population.*

Compensation

For compensation, controls of single stain beads mouse, rat, and REA beads were stained with each appropriate monoclonal antibody depending on their host species or their provider. Specifically, here, REA beads were stained with NKG2A PE, rat beads were stained either with CX3CR1 BUV737 or Ki67 eFluor647, and mouse beads were stained with the other markers. Amine reactive beads were stained with LIVE/DEAD® Fixable Aqua Dead Cell Stain. As it has already been shown in a previously published OMIP, even after the generation of the compensation matrix using each single stain control, a few compensation issues were still observed and were consistent across every experiment (28). Noteworthy, the observed compensation issues were not deemed to be issues as they did not impact the accurate definition of cell population. However, if necessary, in order to correct the visual nuisance, these minor overcompensations can be fixed manually based on comparison to the respective FMO controls or using known marker biology and expression patterns. The three recurrent overcompensation were between CD27 BB660 and Ki67 R660; CD11b PE-Cy5 and CD16 BB660; CD56 PE-Cy5.5 and CD161 BB700.

Empty channel

For detection and exclusion of autofluorescent cells the V510 channel was left empty in this panel. Since the goal of this paper is to define NK cells isolated from tissues where background autofluorescence can be prominent, an empty channel will help to avoid staining issues by gating out autofluorescent events.

Expected variability between individuals

In order to provide an initial assessment of the potential expression variability of the different markers in our panel, we ran the final optimized panel on tumor tissue from four different donors as well as matched-peripheral blood. We quantified the frequency of each marker for two NK cell subsets: NKp46^{+} CD16^{+} and NKp46^{+} CD16^{-} subset (**Online Figure 8).** Our result showed that while some variability is observed across donors, the NK phenotype appears fairly consistent across these donors.

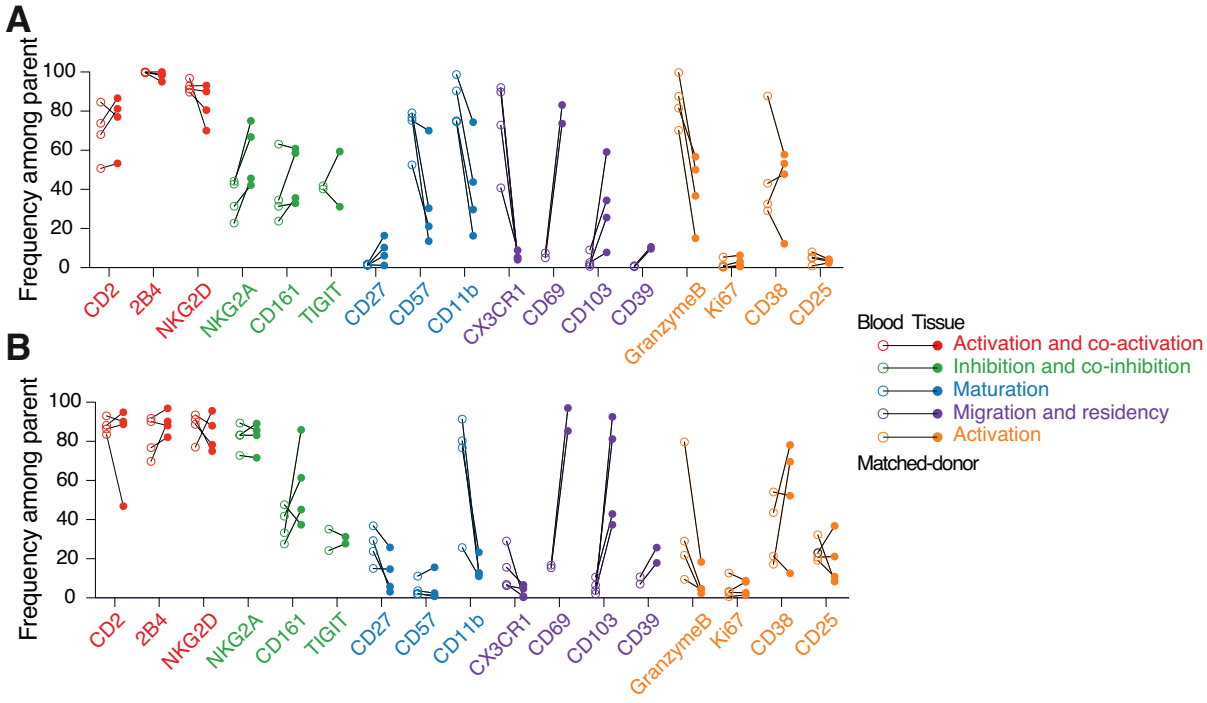

Online Figure 8: Variability of expression among donors

The optimized panel was run on oral squamous cell carcinoma tissues from 4 donors as well as their matched-peripheral blood and the graphs depict the summary statistics for the frequency of the different markers among ***A.*** *NKp46^{+} CD16^{+} and* ***B.*** *NKp46^{+} CD16^{-} NK cells. Blood and tissue from one donor are connected with a black line.*

What about T cells?

While our panel has been designed to provide in-depth characterization of human NK cells isolated from tissue, it can also be used to assess expression of NK-associated markers by T cells (28,36-38) (**Online Figure 9**).

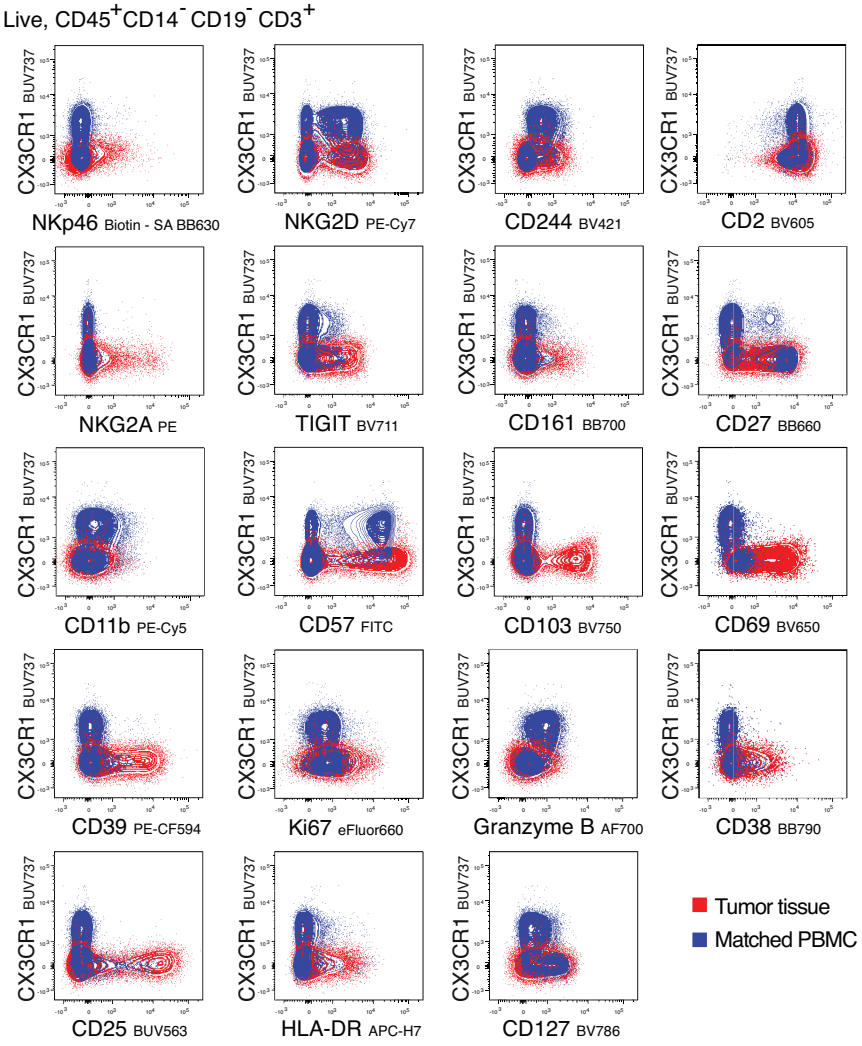

Online Figure 9: Expression of the different markers among the CD3⁺ T cell population

Overview of the 20 phenotypic molecules analyzed within the CD3⁺ T cell compartment of the tumor tissue (red) of a representative donor and its matched-peripheral blood (blue).

Material and Methods

1. Sample preparation

This first section describes the material and method used to prepare single cell suspensions from cryopreserved PBMCs, fresh blood and tumor tissue.

Commercial reagents and materials

- RPMI 1640 (Gibco #11875-093)
- Heat inactivated Fetal Calf Serum (FCS) (Gemini Benchmark #100-106)
- Penicillin-Streptomycin (Gibco #15140-163)
- L-glutamine (Gibco #35050-61)
- Collagenase type II (Sigma #C6885-1G)
- DNase 50U/µL (Sigma #D5025-375KU)
- Petri Dish (Corning #430167)
- Disposable scalpel
- Cell strainers, 70 µm (Falcon #352350)
- 30 cc syringe (BD #302833)
- 16-gauge blunt ended needle (Stem cell #28110)
- 50mL conical tubes
- Lymphoprep™ (StemCell #07851)
- 50 mL tube for density gradient centrifugation SepMate™ (StemCell #85450)

Prepared Buffers

R10 media: RPMI 1640 supplemented with 10% of FCS, 1% of L-glutamine, 1% of Penicillin-Streptomycin

R7.5 media: RPMI 1640 supplemented with 7.5% of FCS, 1% of L-glutamine, 1% of Penicillin-Streptomycin

Collagenase digestion media: in a 50 mL conical tube, warm up 25 mL of R7.5 media for 30 minutes in a 37°C water bath. Prior to the biopsy digestion, add 700 units/mL (number of mg depends on lot) of collagenase type II (based on a titration that was shown to be optimal (39) as well as 2 µL / mL (100 µL in 50 mL) of DNase to prevent cell clumping.

Method

Frozen PBMC:

- Thaw vial in a 37°C water bath
- Slowly dilute in warm R10 media
- Centrifuge at 250 *g* for 5 minutes
- Resuspend in warm R10 media
- Count cells

Blood processing:

- Centrifuge at 400 *g* for 10 minutes
- Remove plasma

- Complete to 35 mL with PBS
- Prepare a 50 mL SepMate™ tube containing 13 mL of Lymphoprep™
- Gently layer blood on top of Lymphoprep™
- Centrifuge at 1200 *g* for 16 minutes with brake off
- Harvest isolated mononuclear cells by pouring the upper layer in a new 50 mL tube
- Wash by adding R10 media
- Centrifuge at 250 *g* for 5 minutes
- Resuspend in R10 media
- Count cells

Tissue processing:

- Cut into smaller pieces with sterile scalpels
- Placed in 50 mL conical tube containing the collagenase digestion media
- Parafilm the lid
- Place tube for 30 minutes of incubation at 37°C with agitation (100-200 rpm)
- Remove from incubator and plunge (at least ten times) with 30 cc syringe and blunt 16-gauge needle
- Pass through a 70 µm strainer into a new 50 ml conical tube and complete with fresh R10 media
- Centrifuge at 250 *g* for 5 minutes
- Resuspend in R10 media
- Count cells

2. Staining protocol

This second section describes the material and method used to stain the different isolated single cells.

Commercial reagents and materials

- Phosphate Buffered Saline PBS (Gibco #20012-027)
- Heat inactivated Fetal Calf Serum (FCS) (Gemini Benchmark #100-106)
- 96-well V-bottom plate
- Brilliant Staining buffer (BD #563794)
- UV Fixable Live/Dead Cell Staining (UV blue, Invitrogen #L34962)
- Fc-Block (BioLegend TruStain FcX #422303)
- CompBeads anti-rat (BD#552844), anti-mouse (BD #552843 and CompBeads Plus #560497), anti-REA (Miltenyi #130-104-693)
- ArC™ Amine Reactive Compensation Bead Kit (Thermo Fisher #A10346)
- Fixation/Dilution Kit: eBioscience™ Foxp3 Transcription Factor Staining Buffer Kit (ThermoFisher #00-5523-00)
- Deionized water (DI H_2O)
- Antibodies used in this panel have been obtained from BD Biosciences, BioLegend, ThermoFisher or Miltenyi as listed in the **Online Table 2** along with the used titers

Prepared Buffers

Staining buffer: PBS supplemented with 2% of FCS

Fc-Block/Viability dye solution: add 25 µL of Fc-Block and 1 µL of reconstituted Live/Dead reagent to 500 µL of PBS immediately prior to use. OMIP-44 has described that the presence of Fc-blocking reagent does not significantly impair the staining of dead cells (5).

Antibody staining mix: add the correct final dilutions of surface antibodies (except streptavidin) in brilliant staining buffer for a final volume of 50 µL per staining.

CompBeads mixes: for anti-Rat and anti-REA compbeads, prepare the mixes by adding 1 drop of negative beads to 1 drop of positive beads for a final volume of 100 µL. For anti-mouse CompBeads, mix 7 drops of the positive and the negative fraction of the CompBeads and CompBeads Plus and complete with 500 µL of staining buffer for a final volume of 1.2 mL.

Streptavidin mix: add the correct final dilution of streptavidin BB630 in staining buffer

Fixation buffer: mix ¼ of concentrate buffer in ¾ of diluent buffer from the Fixation/Dilution Kit

Permeabilization buffer: mix 1/10 of Perm 1x buffer from the Fixation/Dilution Kit in DI H_2O

Intranuclear staining mix: add the correct final dilutions of intracellular (Granzyme B) and intranuclear (Ki67) antibodies in the permeabilization buffer for a final volume of 50 µL per staining

Method

1. Dispensing freshly isolated single cells

- Resuspend cells in the appropriate volume of PBS (Use each sample between 2-5 $\times$ 10^6 cells per staining)

- Dispense into a 96-well V-bottom plate (up to 300 µL)
- Centrifuge plate at 250 *g* for 5 minutes
- Flick supernatant

2. Viability staining

- Resuspend each cell pellets in 100 µL of freshly prepared Fc-Block/Viability solution. At the same time, distribute one drop of the positive beads of the ArC™ compensation kit in an empty well (about 50 µL), and add 0.1 µL of reconstituted Live/Dead reagent.
- Incubate for 15 minutes at room temperature (RT) in the dark (or protect plate with aluminum foil).
- Wash by resuspending in 200 µL of staining buffer
- Centrifuge at 700 *g* for 1 minute.
- Flick supernatant
- Add one drop of the negative beads of the ArC™ compensation kit to well containing the positive beads.

3. Surface staining

- Resuspend each cell pellets in 50 µL of antibody staining mix
- Incubate 20 minutes at RT in the dark
- In parallel, dispense 50 µL of the different CompBeads mixes and add 0.7 µL of a single antibody into each well (0.7 µL is a sufficient quantity for saturating all binding sites on the antibody capture beads for our antibodies and leads to a signal stain as bright or

brighter compared to our experimental samples (data not shown)). Mix and incubate for a minimum of 15 minutes at RT in the dark.

- Wash by resuspending each cell pellets in 200 µL of staining buffer
- Centrifuge at 700 *g* for 1 minute.
- Flick supernatant
- Resuspend in 200 µL of staining buffer
- Centrifuge at 700 *g* for 1 minute.
- Flick supernatant

4. Cytoplasmic and nuclear staining

- Fix cells by resuspending each cell pellets in 150 µL of fixation buffer (same for sample and beads)
- Incubate 40 minutes at 4°C
- Resuspend in 150 µL of permeabilization buffer (same for sample and beads)
- Centrifuge at 700 *g* for 1 minute
- Flick supernatant
- Resuspend in 150 µL of permeabilization buffer (same for sample and beads)
- Centrifuge at 700 *g* for 1 minute
- Flick supernatant
- Resuspend samples in 50 µL of intranuclear staining mix and resuspend beads in 50 µL of permeabilization buffer.
- Incubate 30 minutes at RT in the dark

- Add 150 µL of permeabilization buffer (same for sample and beads)
- Centrifuge at 700 *g* for 1 minute
- Flick supernatant
- Resuspend in 150 µL of permeabilization buffer (same for sample and beads)
- Centrifuge at 700 *g* for 1 minute
- Flick supernatant
- Resuspend the cells and beads in 100 – 200 µL of staining buffer and keep wrapped in aluminum foil at 4°C until acquisition (Samples are acquired between 0 to 5 days after staining. These different timing of acquisition do not affect the staining intensity of the fluorochromes (**Online Figure 10**).

5. Acquire samples on FACSymphony A5

Photomultiplier tube (PMT) voltages were based on prior optimization using voltage titration experiments (5). Each optimized PMT voltage has been assigned to a median fluorescent intensity (MFI) target value based on the peak three, four or five of Ultra Rainbow Particles (Spherotech). These target values were used to calibrate PMT voltages for day-to-day instrument variation (3,40).

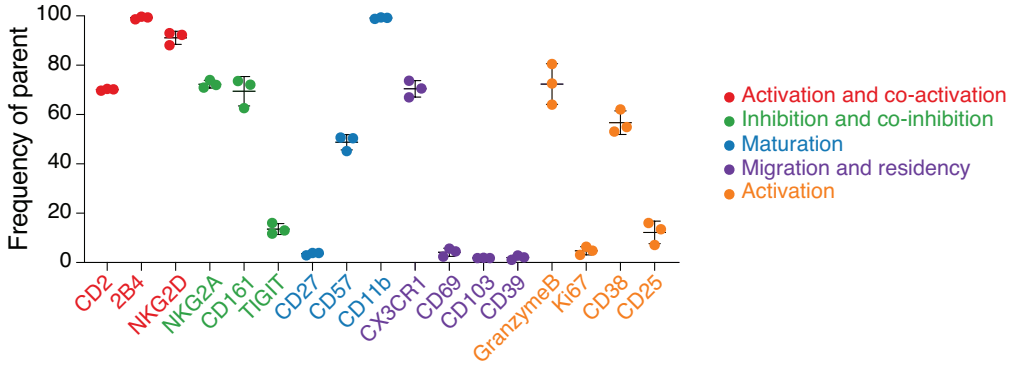

596
597 ***Online Figure 10: Reproducibility of the panel***
598 *Graph showing the frequency of the different markers among NKp46⁺ cells (based on the gating strategy depicted in*
599 *main Figure 1) for PBMC of one healthy donor stained with the 27-color panel and acquired on the FACSymphony A5*
600 *after 0 – 5 days of staining.*
601

602

References

1. Perfetto SP, Chattopadhyay PK, Lamoreaux L, Nguyen R, Ambrozak D, Koup RA, Roederer M. Amine-reactive dyes for dead cell discrimination in fixed samples. Curr Protoc Cytom 2010;Chapter 9:Unit 9 34.
2. Mahnke YD, Roederer M. Optimizing a multicolor immunophenotyping assay. Clin Lab Med 2007;27:469-85, v.
3. Mair F, Tyznik AJ. High-Dimensional Immunophenotyping with Fluorescence-Based Cytometry: A Practical Guidebook. Methods Mol Biol 2019;2032:1-29.
4. Nguyen R, Perfetto S, Mahnke YD, Chattopadhyay P, Roederer M. Quantifying spillover spreading for comparing instrument performance and aiding in multicolor panel design. Cytometry A 2013;83:306-15.
5. Mair F, Prlic M. OMIP-044: 28-color immunophenotyping of the human dendritic cell compartment. Cytometry A 2018;93:402-405.
6. Walzer T, Jaeger S, Chaix J, Vivier E. Natural killer cells: from CD3(-)NKp46(+) to post-genomics meta-analyses. Curr Opin Immunol 2007;19:365-72.
7. Caligiuri MA. Human natural killer cells. Blood 2008;112:461-9.
8. Shemer-Avni Y, Kundu K, Shemesh A, Brusilovsky M, Yossef R, Meshesha M, Solomon-Alemayehu S, Levin S, Gershoni-Yahalom O, Campbell KS and others. Expression of NKp46 Splice Variants in Nasal Lavage Following Respiratory Viral Infection: Domain 1-Negative Isoforms Predominate and Manifest Higher Activity. Front Immunol 2017;8:161.

9. Barrow AD, Edeling MA, Trifonov V, Luo J, Goyal P, Bohl B, Bando JK, Kim AH, Walker J, Andahazy M and others. Natural Killer Cells Control Tumor Growth by Sensing a Growth Factor. Cell 2018;172:534-548 e19.

10. Agresta L, Hoebe KHN, Janssen EM. The Emerging Role of CD244 Signaling in Immune Cells of the Tumor Microenvironment. Front Immunol 2018;9:2809.

11. Liu LL, Landskron J, Ask EH, Enqvist M, Sohlberg E, Traherne JA, Hammer Q, Goodridge JP, Larsson S, Jayaraman J and others. Critical Role of CD2 Co-stimulation in Adaptive Natural Killer Cell Responses Revealed in NKG2C-Deficient Humans. Cell Rep 2016;15:1088-1099.

12. Geary CD, Sun JC. Memory responses of natural killer cells. Semin Immunol 2017;31:11-19.

13. Hammer Q, Romagnani C. OMIP-039: Detection and analysis of human adaptive NKG2C(+) natural killer cells. Cytometry A 2017;91:997-1000.

14. Bjorkstrom NK, Riese P, Heuts F, Andersson S, Fauriat C, Ivarsson MA, Bjorklund AT, Flodstrom-Tullberg M, Michaelsson J, Rottenberg ME and others. Expression patterns of NKG2A, KIR, and CD57 define a process of CD56dim NK-cell differentiation uncoupled from NK-cell education. Blood 2010;116:3853-64.

15. Lazetic S, Chang C, Houchins JP, Lanier LL, Phillips JH. Human natural killer cell receptors involved in MHC class I recognition are disulfide-linked heterodimers of CD94 and NKG2 subunits. J Immunol 1996;157:4741-5.

16. Kurioka A, Cosgrove C, Simoni Y, van Wilgenburg B, Geremia A, Bjorkander S, Sverremark-Ekstrom E, Thurnheer C, Gunthard HF, Khanna N and others. CD161 Defines a Functionally Distinct Subset of Pro-Inflammatory Natural Killer Cells. Front Immunol 2018;9:486.

17. Stanietsky N, Simic H, Arapovic J, Toporik A, Levy O, Novik A, Levine Z, Beiman M, Dassa L, Achdout H and others. The interaction of TIGIT with PVR and PVRL2 inhibits human NK cell cytotoxicity. Proc Natl Acad Sci U S A 2009;106:17858-63.

18. Sun H, Sun C. The Rise of NK Cell Checkpoints as Promising Therapeutic Targets in Cancer Immunotherapy. Front Immunol 2019;10:2354.

19. Judge SJ, Dunai C, Aguilar EG, Vick SC, Sturgill IR, Khuat LT, Stoffel KM, Van Dyke J, Longo DL, Darrow MA and others. Minimal PD-1 expression in mouse and human NK cells under diverse conditions. J Clin Invest 2020.

20. Del Zotto G, Antonini F, Pesce S, Moretta F, Moretta L, Marcenaro E. Comprehensive Phenotyping of Human PB NK Cells by Flow Cytometry. Cytometry A 2020.

21. Hayakawa Y, Smyth MJ. CD27 dissects mature NK cells into two subsets with distinct responsiveness and migratory capacity. J Immunol 2006;176:1517-24.

22. Van Acker HH, Capsomidis A, Smits EL, Van Tendeloo VF. CD56 in the Immune System: More Than a Marker for Cytotoxicity? Front Immunol 2017;8:892.

23. Leong JW, Chase JM, Romee R, Schneider SE, Sullivan RP, Cooper MA, Fehniger TA. Preactivation with IL-12, IL-15, and IL-18 induces CD25 and a functional high-affinity IL-2 receptor on human cytokine-induced memory-like natural killer cells. Biol Blood Marrow Transplant 2014;20:463-73.

24. Lusty E, Poznanski SM, Kwofie K, Mandur TS, Lee DA, Richards CD, Ashkar AA. IL-18/IL-15/IL-12 synergy induces elevated and prolonged IFN-gamma production by ex vivo expanded NK cells which is not due to enhanced STAT4 activation. Mol Immunol 2017;88:138-147.

668 25. Pahl JHW, Koch J, Gotz JJ, Arnold A, Reusch U, Gantke T, Rajkovic E, Treder M, Cerwenka
669 A. CD16A Activation of NK Cells Promotes NK Cell Proliferation and Memory-Like
670 Cytotoxicity against Cancer Cells. Cancer Immunol Res 2018;6:517-527.
671 26. Sabry M, Zubiak A, Hood SP, Simmonds P, Arellano-Ballestero H, Cournoyer E, Mashar M,
672 Pockley AG, Lowdell MW. Tumor- and cytokine-primed human natural killer cells exhibit
673 distinct phenotypic and transcriptional signatures. PLoS One 2019;14:e0218674.
674 27. Le Gars M. SC, Kay A. W., Bayless N. L., Sola E., Starosvetsky E. , Moore L. , Shen-Orr S. S.
675 , Aziz N. , Khatri P. , Dekker C. L., Swan G. E., Davis M. M. , Holmes S. , Blish C. A. . CD38
676 contributes to human natural killer cell responses through a role in immune synapse
677 formation. bioRxiv 2019.
678 28. Liechti T, Roederer M. OMIP-060: 30-Parameter Flow Cytometry Panel to Assess T Cell
679 Effector Functions and Regulatory T Cells. Cytometry A 2019;95:1129-1134.
680 29. Woodward Davis AS, Roozen HN, Dufort MJ, DeBerg HA, Delaney MA, Mair F, Erickson JR,
681 Slichter CK, Berkson JD, Klock AM and others. The human tissue-resident CCR5(+) T cell
682 compartment maintains protective and functional properties during inflammation. Sci
683 Transl Med 2019;11.
684 30. Lugthart G, Melsen JE, Vervat C, van Ostaijen-Ten Dam MM, Corver WE, Roelen DL, van
685 Bergen J, van Tol MJ, Lankester AC, Schilham MW. Human Lymphoid Tissues Harbor a
686 Distinct CD69+CXCR6+ NK Cell Population. J Immunol 2016;197:78-84.
687 31. Spits H, Bernink JH, Lanier L. NK cells and type 1 innate lymphoid cells: partners in host
688 defense. Nat Immunol 2016;17:758-64.

32. Rebuli ME, Pawlak EA, Walsh D, Martin EM, Jaspers I. Distinguishing Human Peripheral Blood NK Cells from CD56(dim)CD16(dim)CD69(+)CD103(+) Resident Nasal Mucosal Lavage Fluid Cells. Sci Rep 2018;8:3394.

33. Castriconi R, Dondero A, Bellora F, Moretta L, Castellano A, Locatelli F, Corrias MV, Moretta A, Bottino C. Neuroblastoma-derived TGF-beta1 modulates the chemokine receptor repertoire of human resting NK cells. J Immunol 2013;190:5321-8.

34. Regis S, Caliendo F, Dondero A, Casu B, Romano F, Loiacono F, Moretta A, Bottino C, Castriconi R. TGF-beta1 Downregulates the Expression of CX3CR1 by Inducing miR-27a-5p in Primary Human NK Cells. Front Immunol 2017;8:868.

35. Simoni Y, Becht E, Fehlings M, Loh CY, Koo SL, Teng KWW, Yeong JPS, Nahar R, Zhang T, Kared H and others. Bystander CD8(+) T cells are abundant and phenotypically distinct in human tumour infiltrates. Nature 2018;557:575-579.

36. Lal KG, Leeansyah E, Sandberg JK, Eller MA. OMIP-046: Characterization of invariant T cell subset activation in humans. Cytometry A 2018;93:499-503.

37. Nettey L, Giles AJ, Chattopadhyay PK. OMIP-050: A 28-color/30-parameter Fluorescence Flow Cytometry Panel to Enumerate and Characterize Cells Expressing a Wide Array of Immune Checkpoint Molecules. Cytometry A 2018;93:1094-1096.

38. Liechti T, Roederer M. OMIP-058: 30-Parameter Flow Cytometry Panel to Characterize iNKT, NK, Unconventional and Conventional T Cells. Cytometry A 2019;95:946-951.

39. McKinnon LR, Hughes SM, De Rosa SC, Martinson JA, Plants J, Brady KE, Gumbi PP, Adams DJ, Vojtech L, Galloway CG and others. Optimizing viable leukocyte sampling from the

female genital tract for clinical trials: an international multi-site study. PLoS One 2014;9:e85675.

40. Perfetto SP, Ambrozak D, Nguyen R, Chattopadhyay PK, Roederer M. Quality assurance for polychromatic flow cytometry using a suite of calibration beads. Nat Protoc 2012;7:2067-79.